

拉曼增益对高双折射光纤中暗孤子俘获的影响

闫青 贾维国 于宇 张俊萍 门克内木乐

Raman effect on dark soliton trapping in high birefringence fiber

Yan Qing Jia Wei-Guo Yu Yu Zhang Jun-Ping Menke Neimule

引用信息 Citation: [Acta Physica Sinica](#), 64, 184211 (2015) DOI: 10.7498/aps.64.184211

在线阅读 View online: <http://dx.doi.org/10.7498/aps.64.184211>

当期内容 View table of contents: <http://wulixb.iphy.ac.cn/CN/Y2015/V64/I18>

您可能感兴趣的其他文章

Articles you may be interested in

[电磁诱导透明系统中的暗孤子](#)

[Dark soliton in the system of electromagnetically induced transparency](#)

物理学报.2015, 64(6): 064202 <http://dx.doi.org/10.7498/aps.64.064202>

[微结构光纤近红外色散波产生的研究](#)

[Study of near-infrared dispersion wave generation for microstructured fiber](#)

物理学报.2015, 64(3): 034215 <http://dx.doi.org/10.7498/aps.64.034215>

[强时间非局域系统中自相位调制诱导的擊齧寰迪駭啁啾](#)

[Inverted-image frequency chirp induced by self-phase modulation in highly noninstantaneous medium](#)

物理学报.2015, 64(2): 024214 <http://dx.doi.org/10.7498/aps.64.024214>

[负性介电各向异性向列相液晶中空间光孤子的理论研究](#)

[Theoretical investigation of spatial optical solitons in nematic liquid crystals with negative dielectric anisotropy](#)

物理学报.2014, 63(18): 184207 <http://dx.doi.org/10.7498/aps.63.184207>

[Hirota 方程的怪波解及其传输特性研究](#)

[Rogue solution of Hirota equation and its transmision](#)

物理学报.2014, 63(10): 104215 <http://dx.doi.org/10.7498/aps.63.104215>

拉曼增益对高双折射光纤中暗孤子俘获的影响*

闫青 贾维国[†] 于宇 张俊萍 门克内木乐

(内蒙古大学物理科学与技术学院, 呼和浩特 010021)

(2015年3月20日收到; 2015年5月6日收到修改稿)

从高双折射光纤中含有拉曼增益的耦合非线性薛定谔方程出发, 利用拉格朗日方法, 推导出了暗孤子俘获的阈值, 并利用快速分步傅里叶变换, 模拟了孤子的两个正交偏振分量的演化, 对比了两种方法得到的阈值, 探究了暗孤子俘获受拉曼增益的影响。研究发现解析解所得阈值比数值解偏小, 且群速度失配越小时, 二者符合得越好; 并且拉曼增益减小了暗孤子的俘获阈值, 当平行拉曼增益增大时, 俘获阈值减小加快。

关键词: 拉曼增益, 暗孤子, 俘获, 高双折射光纤

PACS: 42.65.Tg, 42.65.Dr, 42.65.Jx, 02.30.Nw

DOI: 10.7498/aps.64.184211

1 引言

高双折射光纤中的孤子在交叉相位调制的作用下, 两个正交偏振分量会发生相反方向的频域位移, 慢轴分量蓝移, 快轴分量红移, 导致它们最终以相同的群速度传输, 即孤子自俘获^[1], 这一现象最初是1989年由Islam等^[2]在试验中观察到的。很多研究者尝试从理论上给出孤子俘获的解释, Gorbach和Skryabin^[3,4]在2007年从根本上解释了这一现象。由于光通信技术具有很大的实际应用价值, 孤子俘获吸引了越来越多的研究者^[5–8]。文献[5]研究了锥形光纤中色散波被孤子俘获的现象, 相比于非锥形光纤, 此种光纤的俘获程度更高; He等^[6]探究了孤子在非线性界面的俘获情况; 文献[7, 8]分别研究了光子晶体光纤中色散波被拉曼孤子俘获过程中自陡峭的作用, 以及零色散波长处的蓝移和红移色散波被俘获情况。利用孤子间的相互作用可以实现“开”“关”控制, 并因光孤子本身具有很多优点, 如长距离传输、高容量等, 孤子俘获在全光开关应用上有很大价值, 受到研究者的极大关注^[9–11]。

当输入脉冲的能量较大时, 需要同时考虑两种作用, 即光脉冲与轨道电子和光学声子的相互

作用, 后者引起受激拉曼散射效应产生拉曼增益。拉曼增益对孤子俘获、特别是对暗孤子俘获的影响, 相关研究较少。本文从含有拉曼增益的耦合非线性薛定谔方程(nonlinear Schrödinger equation, NLSE)出发, 推导了包含拉曼增益时暗孤子的自俘获阈值, 并利用快速分步傅里叶变换, 模拟了高双折射光纤中暗孤子的演化, 探讨了拉曼效应、特别是平行拉曼增益对暗孤子俘获的影响。

2 理论模型

加入拉曼增益后, 高双折射光纤中孤子的两个垂直分量 A_x 和 A_y 满足耦合NLSE^[12–14]:

$$\begin{aligned} \frac{\partial A_x}{\partial z} + \beta_{1x} \frac{\partial A_x}{\partial t} + \frac{i}{2} \beta_{2x} \frac{\partial^2 A_x}{\partial t^2} \\ = i \left[\left(\gamma - \frac{ig_0^{||}(\Omega)}{8} \right) |A_x|^2 \right. \\ \left. + \left(\frac{2}{3}\gamma - \frac{ig_0^{\perp}(\Omega)}{4} \right) |A_y|^2 \right] A_x, \end{aligned} \quad (1)$$

$$\begin{aligned} \frac{\partial A_y}{\partial z} + \beta_{1y} \frac{\partial A_y}{\partial t} + \frac{i}{2} \beta_{2y} \frac{\partial^2 A_y}{\partial t^2} \\ = i \left[\left(\gamma - \frac{ig_0^{||}(\Omega)}{8} \right) |A_y|^2 \right. \\ \left. + \left(\frac{2}{3}\gamma - \frac{ig_0^{\perp}(\Omega)}{4} \right) |A_x|^2 \right] A_y, \end{aligned} \quad (2)$$

* 国家自然科学基金(批准号: 61167004)和内蒙古自然科学基金(批准号: 2014MS0104)资助的课题。

† 通信作者。E-mail: jwg1960@163.com

式中, A_x , A_y 代表沿 x , y 方向的慢变包络振幅; β_{1x} 和 β_{1y} 为相应的一阶色散系数; β_{2x} 和 β_{2y} 为二阶色散系数; γ 是非线性系数。 $g_0^{11}(\Omega) = 16i\pi\omega_p^2\chi_{1111}^R(\Omega)/c^2k_pA_p$ 的虚部(即 $ig_0^{11}(\Omega)$ 的实部)代表平行方向拉曼增益, $g_0^\perp(\Omega) = 16i\pi\omega_s^2\chi_{1122}^R/c^2k_sA_{s2}$ 的虚部代表垂直方向拉曼增益。根据 Lin 和 Agrawal [15] 给出的模型, 平行方向拉曼增益较大, 对相关光学过程的影响较大; 垂直拉曼增益相对较小且趋于平稳, 运算中 $g_0^\perp(\Omega)$ 取常数 0.1 m/W。由于实际应用中, 光纤损耗可通过光纤放大器得到补偿, 所以这里忽略了光纤损耗。

对于具有同样波长 λ 的 x , y 分量, 有 $\beta_{2x} = \beta_{2y} = \beta_2$ 。引入归一化振幅 $u = NU$, $v = NV$, $U = A_x/\sqrt{P_0}$, $V = A_y/\sqrt{P_0}$, 归一化时间 $\tau = (t - \bar{\beta}_1 z)/T_0$, 归一化传输距离 $\xi = z/L_D$ 。其中 P_0 为输入脉冲的峰值功率, T_0 为脉冲初始宽度, $\bar{\beta}_1 = (\beta_{1x} + \beta_{1y})/2$, 孤子阶数 $N = \sqrt{L_D/L_{NL}}$, 二阶色散长度 $L_D = T_0^2/|\beta_2|$, 加入拉曼增益的非线性长度 $L_{NL} = 1/\gamma' P_0$, $\gamma' = \gamma - ig_0^{11}(\Omega)/8$ 。方程 (1), (2) 变为标准的耦合 NLSE, 并考虑正常色散区 ($\text{sgn}(\beta_2) = 1$):

$$i\left(\frac{\partial u}{\partial \xi} + \delta \frac{\partial u}{\partial \tau}\right) - \frac{1}{2} \frac{\partial^2 u}{\partial \tau^2} + (|u|^2 + \varepsilon |v|^2)u = 0, \quad (3)$$

$$i\left(\frac{\partial v}{\partial \xi} - \delta \frac{\partial v}{\partial \tau}\right) - \frac{1}{2} \frac{\partial^2 v}{\partial \tau^2} + (|v|^2 + \varepsilon |u|^2)v = 0, \quad (4)$$

式中, $\delta = L_D(\beta_{1x} - \beta_{1y})/2T_0$ 为群速度失配系数, $\varepsilon = \frac{2}{3}\left(1 - \frac{3ig_0^\perp(\Omega)/8 - ig_0^{11}(\Omega)/8}{\gamma'}\right)$ 为加入拉曼增益后线性双折射的耦合参量。

考虑输入脉冲是以偏振角 θ 入射的暗孤子

$$u(0, \tau) = A \cos \theta \tanh(\tau), \quad (5)$$

$$v(0, \tau) = A \sin \theta \tanh(\tau). \quad (6)$$

当两振幅被同等激发时, $\theta = 45^\circ$

$$u(0, \tau) = v(0, \tau) = \frac{A}{\sqrt{2}} \tanh(\tau); \quad (7)$$

当 $\delta = 0$ 时, 方程 (3), (4) 可以简化为下式

$$i\frac{\partial V}{\partial \xi} - \frac{1}{2} \frac{\partial^2 V}{\partial \tau^2} + |V|^2 V = 0, \quad (8)$$

这里 $V = \sqrt{1+\varepsilon}u = \sqrt{1+\varepsilon}v$ 。用逆散射法可得到 (8) 式的解为 [16]

$$V(\xi, \tau) = \eta [B \tanh(\zeta) - i\sqrt{1-B^2}] \exp(i\eta^2 \xi), \quad (9)$$

式中, $\zeta = \eta B(\tau - \tau_s - \eta B\sqrt{1-B^2})$, η 和 τ_s 分别表示背景振幅和下陷的位置。若使 $\xi = 0$ 时下陷中心

位于 $\tau = 0$, 则可设 $\tau_s = 0$ 。 B 决定了下陷深度, 我们考虑黑孤子, 取 $B = 1$, 有

$$u = v = \frac{1}{\sqrt{1+\varepsilon}} \eta \tanh(\eta \tau) \exp(i\eta^2 \xi). \quad (10)$$

振幅 η 和入射脉冲振幅 A 有如下关系 [17]

$$\eta = A \frac{\sqrt{1+\varepsilon}}{\sqrt{2}} - \frac{1}{2}. \quad (11)$$

对于耦合 NLSE, 我们用拉格朗日法

$$\delta \int_{-\infty}^{\infty} d\tau \int_{-\infty}^{\infty} L d\xi = 0. \quad (12)$$

这里拉格朗日量 L 有如下形式

$$L = L_u + L_v + L_{uv}, \quad (13)$$

$$L_u = \frac{i}{2} \left(u^* \frac{\partial u}{\partial \xi} - u \frac{\partial u^*}{\partial \xi} \right) + \frac{i}{2} \delta \left(u^* \frac{\partial u}{\partial \tau} - u \frac{\partial u^*}{\partial \tau} \right) - \frac{1}{2} \left| \frac{\partial u}{\partial \tau} \right|^2 + \frac{1}{2} |u|^4, \quad (14)$$

$$L_v = \frac{i}{2} \left(v^* \frac{\partial v}{\partial \xi} - v \frac{\partial v^*}{\partial \xi} \right) - \frac{i}{2} \delta \left(v^* \frac{\partial v}{\partial \tau} - v \frac{\partial v^*}{\partial \tau} \right) - \frac{1}{2} \left| \frac{\partial v}{\partial \tau} \right|^2 + \frac{1}{2} |v|^4, \quad (15)$$

$$L_{uv} = \varepsilon |u|^2 |v|^2. \quad (16)$$

当两偏振分量间存在耦合时, 相应的解由 (17) 式给出 [18,19]:

$$\begin{bmatrix} u \\ v \end{bmatrix} = \frac{\eta_j}{\sqrt{1+\varepsilon}} \tanh[\eta_j(\tau - M_j)] \times \exp[iC_j(\tau - M_j) + iD_j], \quad (17)$$

系数 $j = 1, 2$ 分别与偏振态 u, v 相对应。参量 η_j, C_j, D_j, M_j 可由欧拉方程确定:

$$\frac{\partial \langle L \rangle}{\partial a} = \frac{d}{d\xi} \left[\frac{\partial \langle L \rangle}{\partial (a/\partial \xi)} \right], \quad (18)$$

其中 a 代表参量 η_j, C_j, D_j, M_j , $\langle L \rangle = \langle L_u \rangle + \langle L_v \rangle + \langle L_{uv} \rangle$, 并定义

$$\langle L \rangle = \int_{-\infty}^{\infty} L d\tau. \quad (19)$$

把 (17) 式代入 (13)–(16) 式计算出 L , 再代入 (18) 和 (19) 式得到

$$\frac{d\eta_j}{d\xi} = 0, \quad (20)$$

$$\frac{dM_j}{d\xi} + (-1)^j \delta - C_j = 0. \quad (21)$$

考虑到 x, y 偏振态的对称性, 有

$$\begin{aligned} \eta_1 &= \eta_2 = \eta, & C_1 &= -C_2 = C, \\ M_{1,2} &= \pm \Delta/4\eta, \end{aligned} \quad (22)$$

其中 Δ 是两个方向暗孤子脉冲最小值的相对距离。把(22)式代入(20)和(21)式得到

$$\frac{d\Delta}{d\xi} = 4\eta\delta + 4\eta C. \quad (23)$$

定义有效势能 $U_{\text{int}}(\Delta) = 4\eta[\langle L_{uv}(0) \rangle - \langle L_{uv}(\Delta) \rangle]$, 则

$$U_{\text{int}}(\Delta) = \frac{16\eta^4}{(1+\varepsilon)^2} \left[\frac{1}{3} - \frac{\cosh \Delta}{\sinh^3 \Delta} (\Delta - \tanh \Delta) \right]. \quad (24)$$

当 $\Delta \rightarrow \infty$ 时得到有效势能的最大值

$$U_{\text{max}} = \frac{16\eta^4}{3(1+\varepsilon)^2}. \quad (25)$$

为了得到孤子俘获的阈值, 这里需要考虑动能

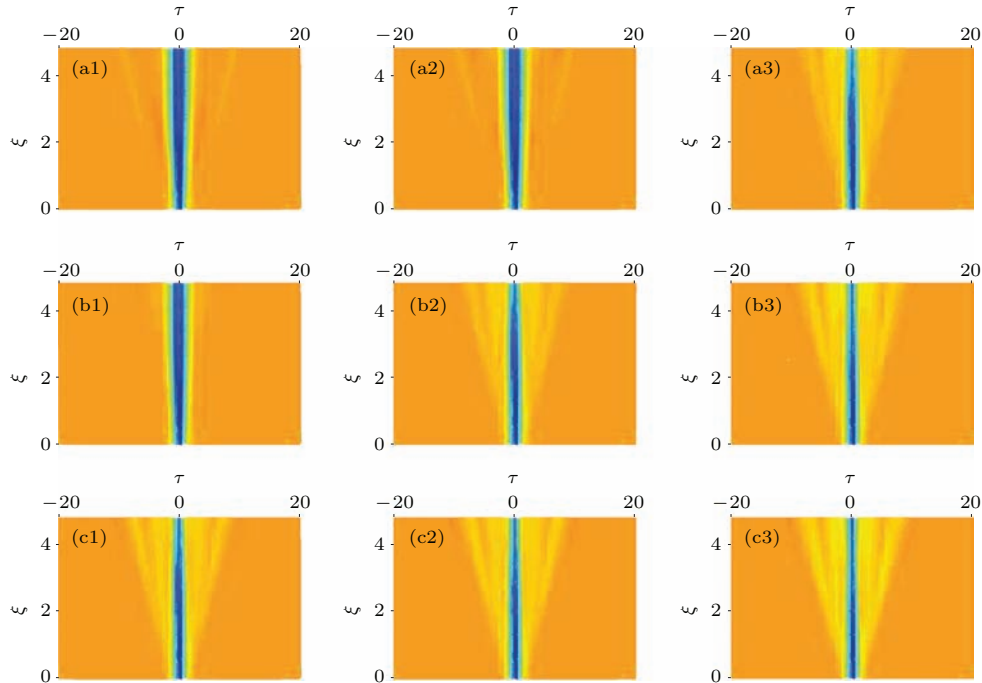
$$E_{\text{kin}} = \frac{1}{2} \left(\frac{d\Delta}{d\xi} \right)^2 \Big|_{\xi=0} = \frac{1}{2} (4\eta\delta)^2,$$

当 $E_{\text{kin}} \leq U_{\text{max}}$ 时, 孤子处于束缚态, 并结合(11)式, 得到暗孤子俘获的阈值

$$A_{\text{th}} = \frac{1}{\sqrt{2(1+\varepsilon)}} + \sqrt{\frac{3(1+\varepsilon)}{\varepsilon}} \delta, \quad (26)$$

ε 为加入拉曼增益后线性双折射的耦合参量。与亮孤子俘获的阈值相比, 暗孤子的阈值较大, 即需要更多的能量才能产生暗孤子自俘获效应。

图1是根据(26)式得到的在不同的群速度失配下, 孤子阈值与平行拉曼增益 $g_0^{/\!/}(\Omega)$ 的关系图。



可以看到, 群速度失配系数越大, 暗孤子的俘获阈值越大; 固定群速度失配系数, 当平行拉曼增益增大时, 暗孤子俘获阈值变小并且变化速度加快。

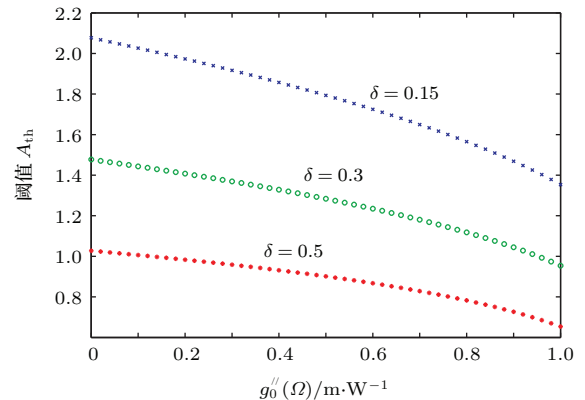


图1 δ 取不同值时, 阈值 A_{th} 随平行拉曼增益的变化

Fig. 1. Change of threshold A_{th} with parallel Raman gain with different δ .

3 数值模拟和分析

取不同的群速度失配系数 δ , 利用快速分步傅里叶变换对(3)式和(4)式进行模拟。

3.1 群速度失配 $\delta = 0.15$

图2是群速度失配系数 $\delta = 0.15$, 输入脉冲振

图2 (网刊彩色) $\delta = 0.15$, A 分别取 0.9, 1, 1.05 时的孤子俘获情况 (对应图(a), (b), (c)) (j1) 不加拉曼效应; (j2) $g_0^{/\!/}(\Omega) = 0.4$; (j3) $g_0^{/\!/}(\Omega) = 0.6$ ($j = a, b, c$)

Fig. 2. (color online) Situation of soliton trapping for $A = 0.9, 1, 1.05$ when $\delta = 0.15$ (corresponding to Fig.2(a), Fig.2(b), Fig.2(c)) (j1) without Raman gain; (j2) $g_0^{/\!/}(\Omega) = 0.4$; (j3) $g_0^{/\!/}(\Omega) = 0.6$ ($j = a, b, c$).

幅取不同值时, 在不含拉曼增益和加入拉曼增益下的孤子俘获情况. 其中, 图2(a)的输入脉冲振幅 $A = 0.9$, 图2(b)的 A 增加到1, 图2(c)的 A 增加到1.05, (j1)为不包含拉曼增益的情况, (j2)为 $g_0^\perp(\Omega) = 0.1 \text{ m/W}$, $g_0^{/\!/}(\Omega) = 0.4 \text{ m/W}$, (j3)为 $g_0^\perp(\Omega) = 0.1 \text{ m/W}$, $g_0^{/\!/}(\Omega) = 0.6 \text{ m/W}$, $j = a, b, c$.

从图2(a)可以看出, 当 $A = 0.9$ 时, 孤子自俘获只发生在平行拉曼增益 $g_0^{/\!/}(\Omega) = 0.6 \text{ m/W}$ 时, 其他两种情况并没有出现; 从图2(b)可以看出, 当 $A = 1$ 时, 孤子自俘获发生在平行拉曼增益 $g_0^{/\!/}(\Omega) = 0.4, 0.6 \text{ m/W}$ 两种情况, 不加拉曼增益时没有发生孤子俘获; 从图2(c)可以看出, 当 $A = 1.05$ 时, 三种情况都发生孤子自俘获. 这说明, 随着平行拉曼增益的增大, 孤子自俘获的阈值越小, 且平行拉曼增益越大, 这种减小会加快, 这与图1所示一致. 通过对(4), (5)两式的模拟, 得到在不包含

拉曼增益、 $g_0^\perp(\Omega) = 0.1 \text{ m/W}$, $g_0^{/\!/}(\Omega) = 0.4 \text{ m/W}$, $g_0^\perp(\Omega) = 0.1 \text{ m/W}$, $g_0^{/\!/}(\Omega) = 0.6 \text{ m/W}$ 三种情况下的阈值分别为1.05, 1和0.9, 这与用(26)式计算得出的阈值0.96, 0.93, 0.87相比略微偏大, 但二者变化趋势基本一致.

3.2 群速度失配 $\delta = 0.3$

图3是群速度失配系数 $\delta = 0.3$, 输入脉冲振幅取不同值时, 在不含拉曼增益和加入拉曼增益下的孤子俘获情况. 其中, 图3(a)的输入脉冲振幅 $A = 1.35$, 图3(b)的 A 增加到1.45, 图3(c)的 A 增加到1.5, (j1)为不包含拉曼增益的情况, (j2)为 $g_0^\perp(\Omega) = 0.1 \text{ m/W}$, $g_0^{/\!/}(\Omega) = 0.4 \text{ m/W}$, (j3)为 $g_0^\perp(\Omega) = 0.1 \text{ m/W}$, $g_0^{/\!/}(\Omega) = 0.6 \text{ m/W}$ ($j = a, b, c$).

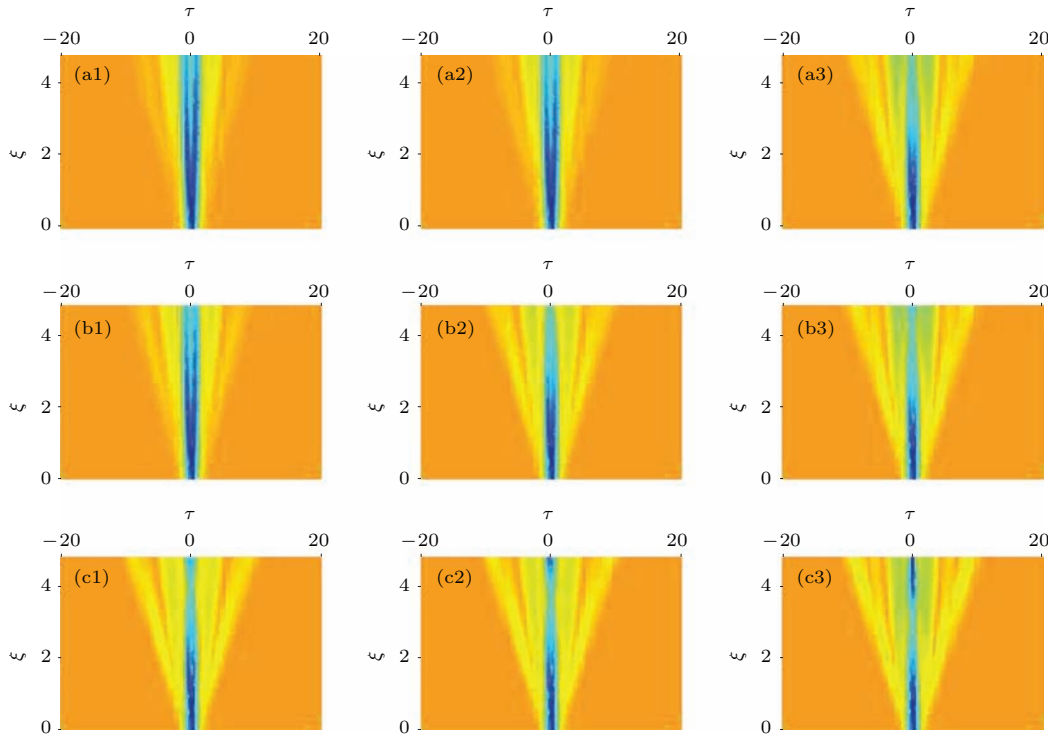


图3 (网刊彩色) $\delta = 0.3$, A 分别取1.35, 1.45, 1.5时的孤子俘获情况 (对应图(a), (b), (c)) (j1) 不加拉曼效应; (j2) $g_0^{/\!/}(\Omega) = 0.4$; (j3) $g_0^{/\!/}(\Omega) = 0.6$ ($j = a, b, c$)

Fig. 3. (color online) Situation of soliton trapping for $A = 1.35, 1.45, 1.5$ when $\delta = 0.3$ (corresponding to Fig.3(a), Fig.3(b), Fig.3(c) (j1) without Raman gain; (j2) $g_0^{/\!/}(\Omega) = 0.4$; (j3) $g_0^{/\!/}(\Omega) = 0.6$ ($j = a, b, c$).

从图3(a)可见, 当 $A = 1.35$ 时, 孤子自俘获只发生在平行拉曼增益 $g_0^{/\!/}(\Omega) = 0.6 \text{ m/W}$ 时, 其他两种情况并没有出现; 从图3(b)可见, 当 $A = 1.45$ 时, 孤子自俘获发生在平行拉曼增益 $g_0^{/\!/}(\Omega) = 0.4, 0.6 \text{ m/W}$ 两种情况, 不加拉曼增益时没有发生孤子俘获; 从图3(c)可见, 当 $A = 1.5$ 时, 三种情况都发生孤子自俘获. 这再次说明, 平行拉曼增益降低了

暗孤子自俘获的阈值, 且平行拉曼增益越大, 孤子自俘获所需的能量越小, 并且这种减小加快. 与计算得到的俘获阈值1.37, 1.33, 1.24相比, 通过傅里叶变换模拟出的暗孤子俘获阈值1.5, 1.45, 1.35相对较大, 且与 $\delta = 0.15$ 时相比, 这种偏差加大. 另外, 对比图2和图3, 随着群速度失配系数的增大, 暗孤子自俘获阈值也增大, 这与图1结果一致.

3.3 群速度失配 $\delta = 0.5$

与图2和图3相比, 图4增大了输入脉冲振幅A的值, 图4(a)的输入脉冲振幅 $A = 2$, 图4(b)的 A 增加到2.1, 图4(c)的 A 继续增加到2.15, (j1)为不包含拉曼效应的情况, (j2)为 $g_0^{\perp}(\Omega) = 0.1 \text{ m/W}$, $g_0^{/\!/}(\Omega) = 0.4 \text{ m/W}$, (j3)为 $g_0^{\perp}(\Omega) = 0.1 \text{ m/W}$, $g_0^{/\!/}(\Omega) = 0.6 \text{ m/W}$, $j = \text{a}, \text{b}, \text{c}$.

可以看到, 由于 δ 的增大, 需要更大能量才能使暗孤子发生自俘获。从图4(a)可见, 当 $A = 2$ 时, 孤子自俘获只发生在平行拉曼增益最大时, 其他两种情况并没有出现; 从图4(b)

可见, 当 $A = 2.1$ 时, 孤子自俘获发生在加入平行拉曼增益后的两种情况; 从图4(c)可见, 当 $A = 2.15$ 时, 三种情况都发生孤子自俘获, 且随着传输距离的增大, 暗孤子的两个正交偏振分量先分开后俘获, 说明它们之间发生了能量交换。通过快速分布傅里叶变换得到不包含拉曼效应, $g_0^{\perp}(\Omega) = 0.1 \text{ m/W}$, $g_0^{/\!/}(\Omega) = 0.4 \text{ m/W}$, $g_0^{\perp}(\Omega) = 0.1 \text{ m/W}$, $g_0^{/\!/}(\Omega) = 0.6 \text{ m/W}$ 三种情况下的阈值分别为2.15, 2.1, 2, 用(26)式计算出的阈值分别为1.92, 1.86, 1.73。相比前两种情况, 这种偏差继续加大, 说明群速度失配系数越小, 计算得到的暗孤子俘获阈值((26)式)符合得越好。

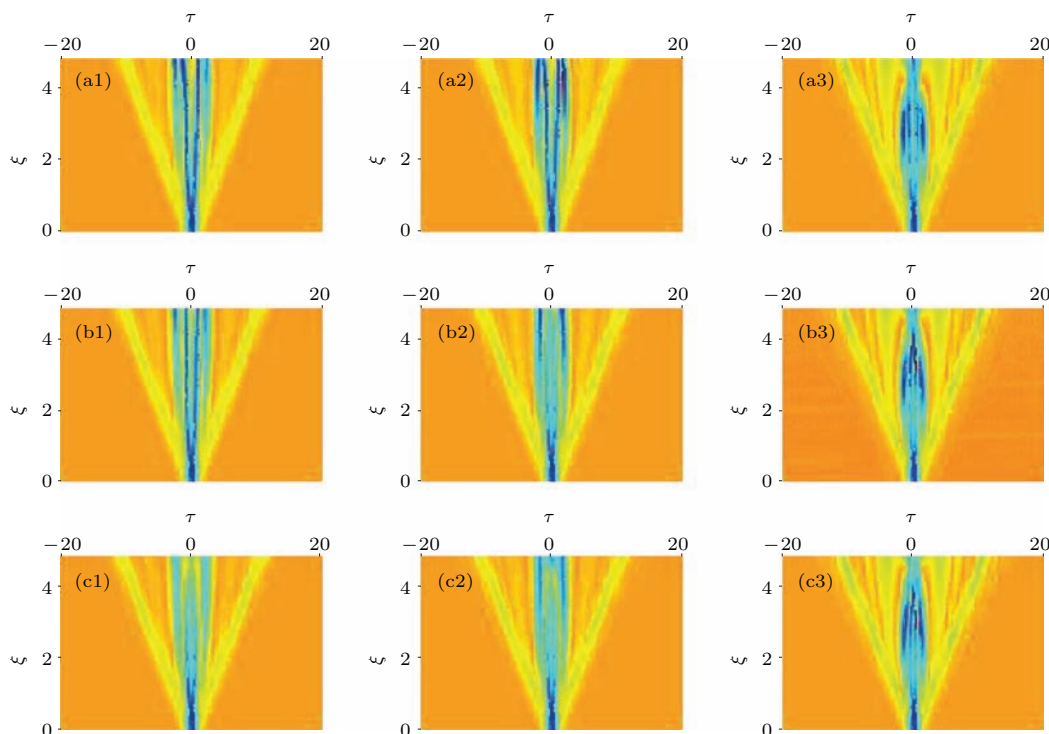


图4 (网刊彩色) $\delta = 0.5$, A 分别取 2, 2.1, 2.15 时的孤子俘获情况 (对应图(a), (b), (c)) (j1) 不加拉曼效应; (j2) $g_0^{/\!/}(\Omega) = 0.4$; (j3) $g_0^{/\!/}(\Omega) = 0.6$ ($j = \text{a}, \text{b}, \text{c}$)

Fig. 4. (color online) Situation of soliton trapping for $A = 2, 2.1, 2.15$ when $\delta = 0.5$ (corresponding to Fig.4(a), Fig.4(b), Fig.4(c)) (j1) without Raman gain; (j2) $g_0^{/\!/}(\Omega) = 0.4$; (j3) $g_0^{/\!/}(\Omega) = 0.6$ ($j = \text{a}, \text{b}, \text{c}$).

4 结 论

本文基于加入拉曼增益的耦合NLSE, 推导出了暗孤子俘获的阈值, 并且利用快速分布傅里叶变换, 模拟了线性高双折射光纤中暗孤子演化。通过对对比两种方法得到的孤子俘获阈值, 解析计算得到的阈值较小, 且群速度失配系数 δ 越小, 这种偏差越小, 说明(26)式在 δ 较小时符合得较好。通过以上分析, 随着群速度失配系数 δ 的增大, 孤子俘

获阈值增大; 当 δ 一定时, 拉曼增益减小了孤子俘获的阈值, 拉曼增益越大, 阈值越小, 并且这种减小趋势越快, 这是解析计算和数值模拟共同得到的结果。

参考文献

- [1] Agrawal G P 2010 *Nonlinear Fiber Optics* (2nd Ed.) (Boston: Academic Press) pp134–165

- [2] Islam M N, Poole C D, Gordon J P 1989 *Opt. Lett.* **14** 1011
- [3] Skryabin D V, Gorbach A V 2007 *Phys. Rev. A* **76** 053803
- [4] Gorbach A V, Skryabin D V 2007 *Nat. Photon.* **1** 653
- [5] Travers J C, Taylor J R 2009 *Opt. Lett.* **34** 115
- [6] He Y J, Mihalache D, Hu B 2010 *Opt. Lett.* **35** 1716
- [7] Liu H Y, Dai Y T, Xu C, Wu J, Xu K, Li Y, Hong X B, Lin J T 2010 *Opt. Lett.* **35** 4042
- [8] Wang W B, Yang H, Tang P H, Han F 2013 *Opt. Express* **21** 11215
- [9] Cheng C, Wang X, Fang Z, Shen B 2005 *Appl. Phys. B* **80** 291
- [10] Zheng L, Tang Y 2010 *Chin. Phys. B* **19** 044209
- [11] Zheng L, Tang Y 2009 *J. Nonlinear Opt. Phys.* **18** 457
- [12] Liu B L, Jia W G, Wang Y P, Qiao H L, Wang X D, Menke N M L 2014 *Acta Phys. Sin.* **63** 214207 (in Chinese) [刘宝林, 贾维国, 王玉平, 乔海龙, 王旭东, 门克内木乐 2014 物理学报 **63** 214207]
- [13] Yu Y, Jia W G, Yan Q, Menke N M L, Zhang J P 2015 *Acta Phys. Sin.* **64** 054207 (in Chinese) [于宇, 贾维国, 闫青, 门克内木乐, 张俊萍 2015 物理学报 **64** 054207]
- [14] Yu Y, Jia W G, Yan Q, Menke N M L, Zhang J P 2015 *Chin. Phys. B* **24** 084210
- [15] Lin Q, Agrawal G P 2006 *Opt. Lett.* **31** 3086
- [16] Agrawal G P 2010 *Nonlinear Fiber Optics* (2nd Ed.) (Boston: Academic Press) pp105–107
- [17] Satsuma J, Yajima N 1974 *Progr. Theor. Phys. Suppl.* **55** 284
- [18] Kivshar Y S 1990 *J. Opt. Soc. Am. B* **7** 2204
- [19] Anderson D, Lisak M 1985 *Phys. Rev. A* **32** 2270

Raman effect on dark soliton trapping in high birefringence fiber*

Yan Qing Jia Wei-Guo[†] Yu Yu Zhang Jun-Ping Menke Neimule

(School of Physical Science and Technology, Inner Mongolia University, Hohhot 010021, China)

(Received 20 March 2015; revised manuscript received 6 May 2015)

Abstract

Not only the interaction between optical pulse and orbital electron but also the interaction between optical pulse and optical phonon needs to be considered when input pulse energy is large. The latter induces the simulated Raman scattering, thus generating the Raman gain. We analyze the effect of Raman gain, especially parallel Raman gain, on dark soliton trapping in high birefringence fiber by analytical method and numerical method. In the first part, we introduce some research results of soliton trapping obtained in recent years. In the second part, the coupled nonlinear Schrödinger equation including Raman gain is utilized for high birefringence fiber. The trapping threshold of dark soliton with considering the Raman gain is deduced by the Lagrangian approach when input pulse is the dark soliton pulse that the amplitude of two polarized components of the dark soliton are the same (see formula (26)). Fig. 1. shows the relation between threshold and parallel Raman gain according to formula (26) when group velocity mismatching coefficient values are 0.15, 0.3, and 0.5 (vertical Raman gains are all 0.1). In the third part, the propagation of the two orthogonal polarization components of dark soliton is simulated by the fractional Fourier transform method. Figures 2–4 show respectively dark soliton trapping with group velocity mismatching coefficient values of 0.15, 0.3 and 0.5. We consider three situations in which Raman gain is not included and the parallel Raman gains are 0.4 and 0.6 when vertical Raman gains are both 0.1 in different group velocity mismatching coefficient values. We obtain the threshold of dark soliton by numerical method under different conditions and analyze the figures. At the same time, we compare the analytical solution with the numerical solution and discuss the effect of Raman gain on dark soliton trapping. The last part focuses on our conclusion. It is found that the threshold which is obtained by analytical method is smaller than that from the numerical solution. The difference between the analytical and numerical dependences decreases with group velocity mismatching coefficient decreases. As a result, formula (26) is in good agreement with numerical data for small group velocity mismatching. The larger the group velocity mismatching, the larger the amplitude threshold of dark soliton is. It also shows that the amplitude threshold of dark soliton can be reduced due to Raman gain and the threshold is reduced faster with the increasing of Raman gain.

Keywords: Raman gain, dark soliton, trapping, high birefringence fiber

PACS: 42.65.Tg, 42.65.Dr, 42.65.Jx, 02.30.Nw

DOI: 10.7498/aps.64.184211

* Project supported by the National Natural Science Foundation of China (Grant No. 61167004), and the Natural Science Foundation of Inner Mongolia, China (Grant No. 2014MS0104).

† Corresponding author. E-mail: jwg1960@163.com